ANALYSIS OF LAMINATED COMPOSITE PLATES BY HYBRID STRESS ISOPARAMETRIC ELEMENT

Y. K. Cheung
Department of Civil and Structural Engineering, University of Hong Kong, Hong Kong

and

Shenglin Di
Department of Civil Engineering, Southeast University, Nanjing, P.R. China

Abstract—A simple quadrilateral hybrid stress element is presented for the analysis of laminated orthotropic and anisotropic plates. The initial trials of layer stresses are pretreated by an energy constraint. A higher-order theory incorporating realistic through thickness approximation of the inplane displacement is proposed. A variety of laminated plate problems are solved and the results are compared with the analytical solution, which demonstrate the validity of the method.

1. INTRODUCTION

The analysis of laminated plates has been of significant concern in many advanced engineering structures. The classical laminated plate theory based on the Kirchhoff hypothesis has been well-established (Reissner and Stavsky, 1961 ; Whitney and Leissa, 1969). Three-dimensional elasticity solutions for some particular plate bending problems have been obtained (Pagano, 1970a,b; Pagano and Hatfield, 1972; Srinivas and Rao, 1970). In the analysis of laminated plates with low span-to-thickness ratios, the classical laminated theory leads to a very poor description of the laminate response, as transverse shear forces become an important role in this case.

For some plates the distortion of the deformed normal due to transverse shear is dependent not only on the plate thickness, but also on the orientation and degree of orthotropic of the individual layer. Accordingly, many plate theories, which include shear deformation, have been proposed (Whitney, 1969; Mau, 1973; Reddy, 1984a,b). Laminated plate elements based on the assumed-displacement model and including transverse shear effects have been developed by many authors (Noor and Rarig, 1974; Greenberg and Stavsky, 1980).

By using the hybrid stress method, which was first established by Pian (Pian, 1964), a laminated thick plate element has been proposed by Mau *et al.*, 1972. Up to now, a number of hybrid/mixed finite element models have appeared in the literature. It has been noticed that the hybrid/mixed finite element exhibits more advantages for laminated plate analysis (Mau *et al.*, 1972; Noor and Anderson, 1977; Reddy and Chao, 1981 ; Spilker, 1982; Liou and Sun, 1987). These include uniform accuracy, convergency for all ranges of shear deformation and excellent prediction of interlaminar stress (Noor and Anderson, 1977). A rational approach to develop hybrid stress elements with additional displacement and an energy constraint has been presented (Wu *et al.*, 1987a). This approach has been implemented in various solid mechanics problems, a series of elements with excellent numerical performance has been developed (Wu *et al.*, 1987a; Di *et al.*, 1989, 1991). General discussion about this new approach has been presented by Pian and Wu, 1988). Due to the fact that the equilibrium condition has not been enforced in the variational principle, the difficulty in choosing equilibrating stress terms no longer exists, so that this approach is very suitable to the analysis of laminated composite plates and shells.

The present study is to develop a hybrid stress element for laminated plate analysis using the approach proposed by Wu *et al.*, 1987a. A higher-order theory (Di, 1992) incorporating realistic through thickness approximation of the inplane displacement is adopted. The layer stresses of this quadrilateral element are optimally constrained by an

energy condition. The validity of the hybrid stress element model developed herein is determined by comparing the numerical results with the existing elasticity analytical solutions.

2. VARIATIONAL FORMULATION

When the additional displacement, denoted by u_λ, is introduced into the Hellinger–Reissner principle, the total displacement can be expressed as the sum of two parts: $u = u_q + u_\lambda$, in which u_q is the compatible displacement interpolated by nodal displacements q. At the same time, we also split the element stress as the sum of two parts: $\sigma = \sigma_c + \sigma_h$, where σ_c and σ_h are the constant part and higher-order part of stress trials, respectively. Due to the discontinuity of the displacement between the interelement boundary, an additional integration corresponding to the energy jump through the element boundary should be included in the variational functional (Pian and Chen, 1982). The modified variational functional for an element consisting of κ layers is in the form (Di, 1988):

$$\Pi^e_{MHR} = \sum_\kappa \int_{V^{e\kappa}} [-\tfrac{1}{2}\sigma^T S\sigma + \sigma^T(Du)]\,dv - \int_{\partial V^{e\kappa}} \sigma^T n u_\lambda \, ds, \tag{1}$$

where S is material matrix, D the differential operator matrix, and n the element stress-traction transformation matrix. The initial higher-order stress trials σ_h can be pretreated by an energy constraint (Wu et al., 1987b; Di, 1992):

$$\int_{\partial V^{e\kappa}} \sigma_h^T n^T u_\lambda \, ds = 0 \quad \text{or} \quad \int_{\partial V^{e\kappa}} u_\lambda^T n \sigma_h \, ds = 0, \tag{2}$$

and denoted as σ_h^*, the final total stress pattern is then obtained by:

$$\sigma^* = \sigma_c + \sigma_h^*. \tag{3}$$

Considering constraint (2) and the pretreated stress trials (3), functional (1) can be simplified as:

$$\Pi^e_{MHR} = \sum_\kappa \int_{V^{e\kappa}} [-\tfrac{1}{2}\sigma^{*T}S\sigma^* + \sigma^{*T}(Du_q) + \sigma_h^{*T}(Du_\lambda)]\,dv. \tag{4}$$

According to the selecting of incompatible displacement (Wu and Bufler, 1990), the base functions in the incompatible displacements u_λ should be independent from the one already used in the compatible displacements u_q. In this case, the incompatible displacements are usually the higher-order part of the total displacement. Due to the fact that σ_h^* is also the higher-order part of the stress trials, the virtual work done by σ_h^* to the strain derived from u_λ is a higher-order term of the energy functional and can be neglected. Hence the modified Hellinger–Reissner functional can be further simplified as:

$$\Pi^e_{MHR} = \sum_\kappa \int_{V^{e\kappa}} [-\tfrac{1}{2}\sigma^{*T}S\sigma^* + \sigma^{*T}(Du_q)]\,dv. \tag{5}$$

It is worthwhile to note that the incompatible displacements do not appear in the modified functional (5) and are only used for the pretreatment of initial stress trials in eqn (2). The element obtained by such an approach is still a compatible model.

In order to determine the higher-order stresses which satisfy constraint (2), the initial higher-order stresses are defined as:

$$\sigma_h = [\Phi_I \Phi_{II}] \begin{Bmatrix} \beta_I \\ \beta_{II} \end{Bmatrix}, \tag{6}$$

where $\mathbf{\Phi}_i$ and β_i are the interpolation matrix and stress parameter vector, respectively. The additional displacement field is expressed in terms of internal parameters λ through the shape function matrix $\mathbf{N}_\lambda$:

$$\mathbf{u}_\lambda = \mathbf{N}_\lambda \lambda. \tag{7}$$

Substituting eqns (6) and (7) into eqn (2) yields:

$$\lambda^{\mathrm{T}}[\mathbf{M}_{\mathrm{I}}\mathbf{M}_{\mathrm{II}}] \begin{Bmatrix} \beta_{\mathrm{I}} \\ \beta_{\mathrm{II}} \end{Bmatrix} = 0. \tag{8}$$

where

$$\mathbf{M}_{\mathrm{I}} = \int_{\partial V^{e\kappa}} \mathbf{N}_\lambda^{\mathrm{T}} \mathbf{n} \mathbf{\Phi}_{\mathrm{I}} \, \mathrm{d}s, \quad \mathbf{M}_{\mathrm{II}} = \int_{\partial V^{e\kappa}} \mathbf{N}_\lambda^{\mathrm{T}} \mathbf{n} \mathbf{\Phi}_{\mathrm{II}} \, \mathrm{d}s. \tag{8a}$$

Due to the arbitrary nature of parameters λ, the stress parameters β_{II} in equation (8) can be expressed in terms of β_{I}:

$$\beta_{\mathrm{II}} = -\mathbf{M}_{\mathrm{II}}^{-1} \mathbf{M}_{\mathrm{I}} \beta_{\mathrm{I}}. \tag{9}$$

Replacing β_{II} in eqn (6) by eqn (9), the pretreated version of higher-order stresses σ_{h}^* will be in the form:

$$\sigma_{\mathrm{h}}^* = [\mathbf{\Phi}_{\mathrm{I}} - \mathbf{\Phi}_{\mathrm{II}} \mathbf{M}_{\mathrm{II}}^{-1} \mathbf{M}_{\mathrm{I}}] \beta_{\mathrm{I}}. \tag{10}$$

The total layer stresses are then obtained by:

$$\sigma^* = \mathbf{I}_5 \beta_{\mathrm{c}} + \mathbf{\Phi}_{\mathrm{h}}^* \beta_{\mathrm{I}} = \mathbf{\Phi}^* \beta^*, \tag{11}$$

in which

$$\left. \begin{aligned} \mathbf{\Phi}^* &= [\mathbf{I}_5 \mathbf{\Phi}_{\mathrm{h}}^*], \quad \mathbf{\Phi}_{\mathrm{h}}^* = \mathbf{\Phi}_{\mathrm{I}} - \mathbf{\Phi}_{\mathrm{II}} \mathbf{M}_{\mathrm{II}}^{-1} \mathbf{M}_{\mathrm{I}} \\ \mathbf{I}_5 &\text{ denotes a five order matrix} \\ \beta_{\mathrm{c}} &= [\beta_1 \beta_2 \ldots \beta_5]^{\mathrm{T}} \\ \beta^* &= \begin{Bmatrix} \beta_{\mathrm{c}} \\ \beta_{\mathrm{I}} \end{Bmatrix} \end{aligned} \right\}. \tag{11a}$$

It is noted that the inverse $\mathbf{M}_{\mathrm{II}}^{-1}$ always exists for an arbitrary configuration as long as $\mathbf{\Phi}_{\mathrm{II}}$ has been carefully selected. In other words, there is no difficulty in obtaining the stress pattern σ^* by following the above procedure.

The displacement field $\mathbf{u}_q$ can be interpolated from nodal displacement $\mathbf{q}$:

$$\mathbf{u}_q = \mathbf{N}_q \mathbf{q}, \tag{12}$$

and the strain corresponding to displacement $\mathbf{u}_q$ can be calculated by using the linear strain–displacement relationship as:

$$\varepsilon = \mathbf{D}\mathbf{u}_q = \mathbf{D}\mathbf{N}_q \mathbf{q} = \mathbf{B}\mathbf{q}. \tag{13}$$

Finally, substituting eqns (11)–(13) into eqn (5) yields:

$$\Pi_{\mathrm{MHR}}^e = \sum_\kappa (-\tfrac{1}{2} \beta_\kappa^{\mathrm{T}} \mathbf{H}_\kappa \beta_\kappa + \beta_\kappa^{\mathrm{T}} \mathbf{G}_\kappa \mathbf{q}), \tag{14}$$

in which

$$H_\kappa = \int_{V^{e\kappa}} \Phi_\kappa^T S_\kappa \Phi_\kappa \, dV$$

$$G_\kappa = \int_{V^{e\kappa}} \Phi_\kappa^T B_{q\kappa} \, dV \qquad \left.\right\} \qquad (14a)$$

Taking a variation of equation (14) yields the following stiffness matrix for the whole laminate element:

$$K^e = \sum_\kappa K_\kappa = \sum_\kappa G_\kappa^T H_\kappa^{-1} G_\kappa. \tag{15}$$

3. DISPLACEMENT AND STRESS TRIALS

Consider the multilayered plate element composed of N perfectly bonded laminae as shown in Fig. 1, where z corresponds to the transverse direction of the laminate. To achieve the general applicability, an isoparametric finite element formulation is adopted, which expresses the element coordinates, displacements and stresses through the natural coordinates.

A number of laminated plate theories have been proposed based on Mindlin's hypothesis of normals remaining straight, but not necessarily normal, to the midsurface after deformation. While these theories are quite accurate for the estimation of global characteristics like deflections, fundamental frequency and buckling load, they have been shown
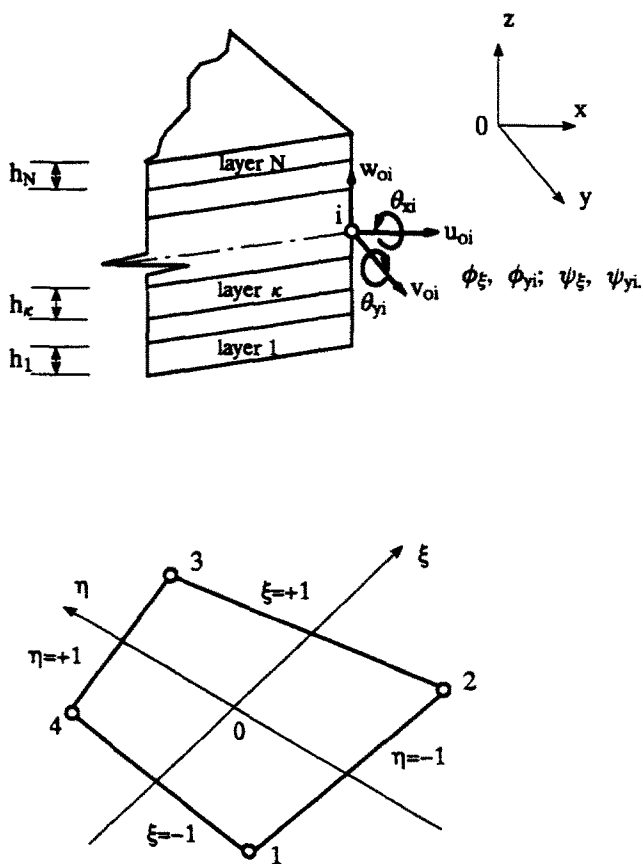

Fig. 1. Coordinate systems of laminated plate element (a) nodal i of a laminate element, (b) natural coordinates.

to be inadequate for the estimation of higher-order frequencies, mode shape and distribution of displacements and stresses across the plate thickness. Furthermore, they require an arbitrary shear correction to the transverse shear stiffnesses.

A remedy from the three-dimensional elasticity solution (Pagano, 1970a,b) is to include a cubic term and a zig-zag function for the inplane displacements u and v, so that a satisfactory distribution of the displacements and stresses can be achieved. These portions are specially important for simulating the strong warping phenomenon that exists in thicker or anisotropic laminates. We begin with the following through-thickness displacement distribution:

$$\begin{Bmatrix} u \\ v \end{Bmatrix}^{\kappa} = \begin{Bmatrix} u_o \\ v_o \end{Bmatrix} + z \begin{Bmatrix} \theta_x \\ \theta_y \end{Bmatrix} + z^3 \begin{Bmatrix} \phi_x \\ \phi_y \end{Bmatrix} + \hat{z} \begin{Bmatrix} \psi_x \\ \psi_y \end{Bmatrix}, \\ w^{\kappa} = w_o$$ \right\} \tag{16}$$

where the superscript κ refers to the κth layer; u_o, v_o and w_o are the displacement of midsurface, θ_x and θ_y are the normal rotation of the midsurface for the whole laminate to the x and y axis, respectively, ϕ_x and ϕ_y the parameter of cubic function and ψ_x and ψ_y the layer normal rotation. All these unknown nodal variables are the functions of isoparametric coordinates ξ, η only, and their geometrical illustrations are shown in Fig. 2; $\hat{z}$ is a piecewise linear, C^o continuous zig-zag function. If the midsurface of the laminated plate is located in the Lth layer, $\hat{z}$ can be expressed as:

$$\hat{z} = \sum_{i=1}^{\kappa-1} (-1)^i h_i + (-1)^{\kappa} (1+\zeta) \frac{h_{\kappa}}{2} \hat{z}_L, \tag{17}$$

where

$$\hat{z}_L = \sum_{i=1}^{L-1} (-1)^i h_i + (-1)^L z_o, \tag{17a}$$

and z_o is the distance between the laminate midsurface and the lower surface of the Lth layer, as illustrated in Fig. 2, h_i the thickness of layer i and ζ the layer natural coordinate which takes -1 and $+1$ at the lower and upper surface of each layer.

For the most commonly used laminates, the lamination sequences are symmetric about the midsurface, the absent z^2 term in the expression (16) for inplane displacements u and v
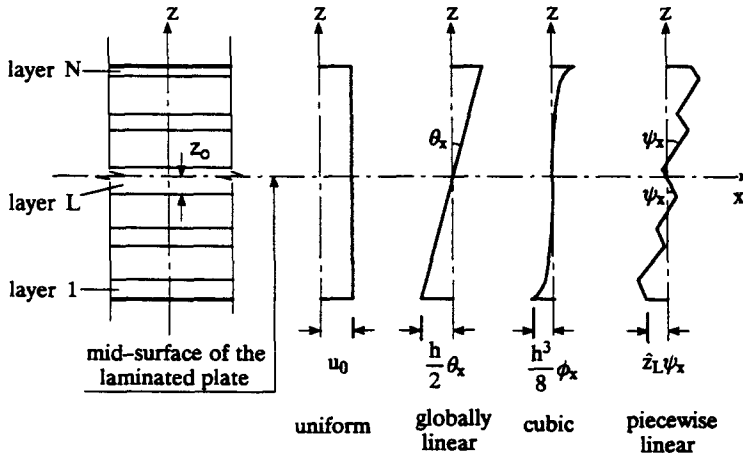

Fig. 2. Illustration of the inplane displacement of higher-order theory.

has negligible influence on the results of analysis in this case. However, such a term should be included for the more general case of unsymmetric laminates.

Only for single layer plate, the second term (global linear part) and last term (piecewise linear part) have the same physical interpretation, but usually their influences for multi-layered plates are quite different. Because the distribution of inplane displacement for each layer is approximately linear in the case of the laminates consisting of a number of layers, the cubic term of eqn (16) can be neglected to reduce the element degree of freedom. In addition, the influence of both the cubic term and the zig-zag function will be negligible if the span–thickness ratio of the laminated plate is very large. This characteristic will be illustrated by the numerical example in the subsequent section. It is worthwhile to use eqn (16) to develop the element model for the general purpose analysis.

For the four-node quadrilateral element shown in Fig. 1, the bilinear interpolating function $N_i = (1 + \xi_i\xi)(1 + \eta_i\eta)/4$ is used in terms of the isoparametric coordinates ξ and η. The strain–displacement relation of the higher-order theory for each layer can be expressed as:

$$\boldsymbol{\varepsilon} = \begin{Bmatrix} \varepsilon_x \\ \varepsilon_y \\ \varepsilon_{xy} \\ \varepsilon_{yz} \\ \varepsilon_{zx} \end{Bmatrix} = [\mathbf{B}_1\mathbf{B}_2\mathbf{B}_3\mathbf{B}_4] \begin{Bmatrix} \mathbf{q}_1 \\ \mathbf{q}_2 \\ \mathbf{q}_3 \\ \mathbf{q}_4 \end{Bmatrix} = \mathbf{Bq}, \tag{18}$$

where $\mathbf{q}_i$ is the generalized displacement of node i:

$$\mathbf{q}_i = [u_{oi} v_{oi} w_{oi} \theta_{xi} \theta_{yi} \phi_{xi} \phi_{yi} \psi_{xi} \psi_{yi}]^\mathrm{T}. \tag{19}$$

The total number of nodal displacements for a laminated plate element is 36 and independent from the the total number of layers. The submatrix $\mathbf{B}_i$ can be expressed as:

$$\mathbf{B}_i = \begin{bmatrix} N_{i,x} & 0 & 0 & zN_{i,x} & 0 & z^3N_{i,x} & 0 & \hat{z}N_{i,x} & 0 \\ 0 & N_{i,y} & 0 & 0 & zN_{i,y} & 0 & z^3N_{i,y} & 0 & \hat{z}N_{i,y} \\ N_{i,y} & N_{i,x} & 0 & zN_{i,y} & zN_{i,x} & z^3N_{i,y} & z^3N_{i,x} & \hat{z}N_{i,y} & \hat{z}N_{i,x} \\ 0 & 0 & N_{i,y} & 0 & N_i & 0 & 3z^2N_i & 0 & (-1)^\kappa N_i \\ 0 & 0 & N_{i,x} & N_i & 0 & 3z^2N_i & 0 & (-1)^\kappa N_i & 0 \end{bmatrix}, \tag{20}$$

in which we have introduced the following relations:

$$\left. \begin{aligned} z &= \sum_{i=1}^{\kappa-1} h_i + (1+\zeta)\frac{h_\kappa}{2} - \frac{h}{2} \\ \frac{\partial}{\partial z} &= \frac{2}{h_\kappa}\frac{\partial}{\partial \zeta} \end{aligned} \right\} . \tag{21}$$

Each layer of the laminated composite element is assumed to be generally orthotropic or anisotropic with an elastic symmetry plane perpendicular to the z axis.

The incompatible displacement is assumed as:

$$\mathbf{u}_\lambda = \begin{Bmatrix} u \\ v \\ w \end{Bmatrix}_\lambda = \begin{bmatrix} \xi^2 & \eta^2 & 0 & 0 & 0 & 0 \\ 0 & 0 & \xi^2 & \eta^2 & 0 & 0 \\ 0 & 0 & 0 & 0 & \xi^2 & \eta^2 \end{bmatrix} \begin{Bmatrix} \lambda_1 \\ \lambda_2 \\ \vdots \\ \vdots \\ \lambda_6 \end{Bmatrix} = \mathbf{N}_\lambda \boldsymbol{\lambda}. \tag{22}$$

The initial stress of each layer is defined by:

$$\sigma = \begin{Bmatrix} \sigma_x \\ \sigma_y \\ \sigma_{xy} \\ \sigma_{yz} \\ \sigma_{zx} \end{Bmatrix} = \begin{Bmatrix} \beta_1 \\ \beta_2 \\ \vdots \\ \vdots \\ \beta_5 \end{Bmatrix} + [\Phi_I \Phi_{II}] \begin{Bmatrix} \beta_6 \\ \vdots \\ \beta_{30} \\ \beta_{31} \\ \vdots \\ \beta_{36} \end{Bmatrix} = \beta_c + [\Phi_I \Phi_{II}] \begin{Bmatrix} \beta_I \\ \beta_{II} \end{Bmatrix}, \tag{23}$$

where

$$\Phi_I =$$

$$\begin{bmatrix} \eta & \zeta & \xi\zeta & \eta\zeta & \zeta^2 & 0 & 0 & 0 & 0 & 0 & 0 & 0 & 0 & 0 & 0 & 0 & 0 & 0 & 0 & 0 & 0 & 0 & 0 & 0 & 0 \\ 0 & 0 & 0 & 0 & 0 & \xi & \zeta & \xi\zeta & \eta\zeta & \zeta^2 & 0 & 0 & 0 & 0 & 0 & 0 & 0 & 0 & 0 & 0 & 0 & 0 & 0 & 0 & 0 \\ 0 & 0 & 0 & 0 & 0 & 0 & 0 & 0 & 0 & 0 & \xi\eta & \zeta & \xi\zeta & \eta\zeta & \zeta^2 & 0 & 0 & 0 & 0 & 0 & 0 & 0 & 0 & 0 & 0 \\ 0 & 0 & 0 & 0 & 0 & 0 & 0 & 0 & 0 & 0 & 0 & 0 & 0 & 0 & 0 & \xi & \zeta & \xi\zeta & \eta\zeta & \zeta^2 & 0 & 0 & 0 & 0 & 0 \\ 0 & 0 & 0 & 0 & 0 & 0 & 0 & 0 & 0 & 0 & 0 & 0 & 0 & 0 & 0 & 0 & 0 & 0 & 0 & 0 & \eta & \zeta & \xi\zeta & \eta\zeta & \zeta^2 \end{bmatrix}$$

$$\Phi_{II} = \begin{bmatrix} \xi & 0 & 0 & 0 & 0 & 0 \\ 0 & \eta & 0 & 0 & 0 & 0 \\ 0 & 0 & \xi & \eta & 0 & 0 \\ 0 & 0 & 0 & 0 & \eta & 0 \\ 0 & 0 & 0 & 0 & 0 & \xi \end{bmatrix} \tag{23a}$$

For the initial stress trials corresponding to a bilinear displacement interpolation, it is reasonable to select a polynomial which is complete linear in the plane coordinates ξ and η. In addition, the strains derived from the displacement trial (16) will be of second order of the transverse coordinate ζ, it is suitable to include the ζ^2 in the stress trial (23), according to the matching condition of dual variables (Wu and Bufler, 1990). It should be noted that the matrix Φ_{II} has been carefully selected in order to guarantee the existence of M_{II}^{-1}, see eqn (9). In addition, the following condition:

$$\text{dim.}(\beta_{II}) = \text{dim.}(\lambda), \tag{24}$$

has also been considered so that enough constraint equations can be obtained to eliminate β_{II} from eqn (2). Because β_{II} will be eliminated by constraint (2), the final stress parameters consist only of β_c and β_I, the parameter-control condition (Pian and Wu, 1988):

$$\text{dim.}(\beta^*) = \text{dim.}(q) - r = 36 - 6 = 30, \tag{25}$$

has been satisfied.

4. EXAMPLE PROBLEMS AND NUMERICAL RESULTS

To test the validity of the finite element analysis technique and to establish its range of applicability, several numerical examples are investigated. Comparisons were made with analytical converged solutions as well as the results obtained by the classical laminate theory or other finite element models. The results for the present method are taken directly from the specified positions without any stress smoothing technique.

The boundary conditions used for the following examples are specified in terms of the generalized nodal displacements, as shown in Table 1. All the problems studied in this paper

Table 1. Boundary conditions

Type of restraint	Conditions along $x =$ constant	Conditions along $y =$ constant
Simply supported	$v_o = w_o = \theta_y = \phi_y = \psi_y = 0$	$u_0 = w_0 = \theta_x = \phi_x = \psi_x = 0$
Clamped	All displacements are zero	All displacements are zero
Free	All displacements are free	All displacements are free
Symmetric line	$u_o = \theta_x = \phi_x = \psi_x = 0$	$v_o = \theta_y = \phi_y = \psi_y = 0$

are symmetric cross-ply or angle-ply laminates. The boundary conditions listed in Table 1 are imposed at the edge of the example plates by considering the corresponding conditions used for the three dimensional elasticity solution (Pagano, 1970a,b). In case of doubt the entire plate model has been used, for example in example 4.3 for the angle-ply laminate. However, it is worthwhile to note that the type of simply supported boundary conditions used for unsymmetric cross-ply and angle-ply laminates should be different (Reddy, 1984a,b).

4.1. *Bending of rectangular plates* (0/90/0, b = 3a)

A simply-supported rectangular laminated plate with three layers of equal thickness is considered here, as shown in Fig. 3. The subjected transverse loading is sinusoidally distributed and defined as :

$$q(x, y) = q_0 \sin \frac{\pi x}{a} \sin \frac{\pi y}{b}. \tag{26}$$

The lamina properties are assumed to be

$$E_L = 25 \times 10^6, \qquad E_T = 10^6,$$

$$G_{LT} = 0.5 \times 10^6, \qquad G_{TT} = 0.2 \times 10^6,$$

$$\nu_{LT} = \nu_{TT} = \nu_{TL} = 0.25, \tag{27}$$

where L signifies the fiber direction, T the transverse direction. To validate the accuracy of the present method, the results are compared with the three-dimensional elasticity solutions of Pagano (1970a,b). The predicted results of stresses and displacements are listed in Table 2 for different span–thickness ratios ($S = a/h = 4, 10, 20, 100$). The following normalized
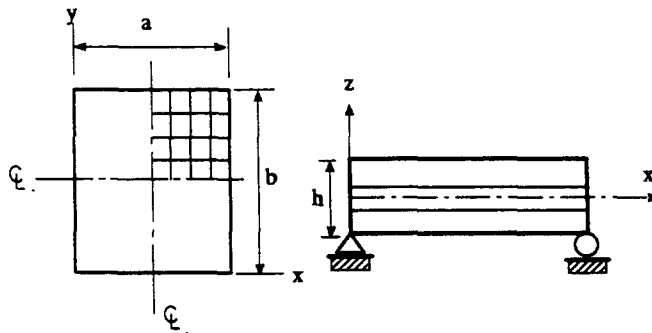

Fig. 3. Bending of a simply-supported rectangular laminated plate under sinusoidal loading.

Table 2. Nondimensionalized deflections and stresses in three layer cross-ply (0/90/0) rectangular ($b = 3a$) laminate under sinusoidal loading[†]

$S = \dfrac{a}{h}$	Source	$\bar{w}\left(\dfrac{a}{2},\dfrac{a}{2},0\right)$	$\bar{\sigma}_{11}\left(\dfrac{a}{2},\dfrac{a}{2},\dfrac{h}{2}\right)$	$\bar{\sigma}_{22}\left(\dfrac{a}{2},\dfrac{a}{2},\dfrac{h}{4}\right)$	$\bar{\sigma}_{12}\left(0,0,\dfrac{h}{2}\right)$	$\bar{\sigma}_{23}\left(\dfrac{a}{2},0,0\right)$	$\bar{\sigma}_{31}\left(0,\dfrac{a}{2},0\right)$
4	Pagano	2.8200	1.1000	0.1190	0.0281	0.0334	0.3870
	HSDT	2.6411	1.0356	0.1028	0.0263	0.0348	0.2724
	Liou	2.8280	1.0770	0.1080	0.0267	0.0326	0.3600
	Present	2.8370	1.0960	0.1110	0.0273	0.0299	0.3532
10	Pagano	0.919	0.7250	0.0435	0.0123	0.0152	0.420
	HSDT	0.862	0.6924	0.0398	0.0115	0.0170	0.2859
	Liou	0.9210	0.7090	0.0429	0.0121	0.0151	0.4280
	Present	0.920	0.7200	0.0418	0.1200	0.0144	0.4249
20	Pagano	0.6100	0.6500	0.0299	0.0093	0.0119	0.4340
	HSDT	0.5937	0.6407	0.0289	0.0091	0.0130	0.2880
	Liou	0.6110	0.6530	0.0298	0.0093	0.0118	0.4500
	Present	0.6086	0.6457	0.0293	0.0092	0.0116	0.4393
100	Pagano	0.5080	0.624	0.0253	0.0083	0.0108	0.439
	HSDT	0.5070	0.624	0.0253	0.0083	0.0129	0.2886
	Present	0.5061	0.620	0.0252	0.0082	0.0106	0.4442
	CLT	0.503	0.623	0.0252	0.0083	—	—

[†] Note that this form is drawn from (Reddy, 1984a,b), Pagano's elasticity analytical solution (Pagano, 1970a,b), present hybrid stress shell element (6 × 12 mesh). HSDT (simple higher-order theory) (Reddy, 1984a,b), Liou three dimensional hybrid element (Liou *et al.*, 1987) and CLT (classical laminate theory).

quantities employed by Pagano (1970a,b) are also adopted here :

$$(\bar{\sigma}_x, \bar{\sigma}_y, \bar{\sigma}_{xy}) = \frac{h^2}{q_o a^2}(\sigma_x, \sigma_y, \sigma_{xy}),$$

$$(\bar{\sigma}_{yz}, \bar{\sigma}_{zx}) = \frac{h}{q_o a}(\sigma_{yz}, \sigma_{zx}),$$

$$\bar{u} = \frac{E_T h^2}{q_o a^3}u, \quad \bar{w} = \frac{100 \times E_T h^3}{q_o a^4}w. \tag{28}$$

Owing to symmetry, only a quarter of the plate is used for finite element analysis with 6 × 12 mesh. The results obtained by Reddy (1984a,b) using a simple higher-order theory,

Table 3. Maximum stresses and deflection in three-ply (0/90/0) laminate under sinusoidal loading[†]

$S = \dfrac{a}{h}$	Source	$\bar{\sigma}_x\left(\dfrac{a}{2},\dfrac{a}{2},\pm\dfrac{h}{2}\right)$	$\bar{\sigma}_y\left(\dfrac{a}{2},\dfrac{a}{2},\pm\dfrac{h}{4}\right)$	$\bar{\sigma}_{xz}\left(0,\dfrac{a}{2},0\right)$	$\bar{\sigma}_{yz}\left(\dfrac{a}{2},0,0\right)$	$\bar{\sigma}_{xy}\left(0,0,\pm\dfrac{a}{2}\right)$	$\bar{w}\left(\dfrac{a}{2},\dfrac{a}{2},0\right)$
4	Pagano	0.720	0.663	0.219	0.292	−0.0467	4.491
		−0.684	−0.666	0.222(−0.27)		0.0458	
	Present	±0.690	±0.622	0.225	0.254	∓0.046	4.490
10	Pagano	±0.559	0.401	0.301	0.196	−0.0275	1.709
			−0.403			0.0276	
	Present	±0.555	±0.396	0.310	0.164	∓0.0273	1.696
20	Pagano	±0.543	0.308	0.328	0.156	∓0.0230	1.189
			−0.309				
	Present	±0.540	±0.306	0.338	0.130	∓0.0228	1.178
100	Pagano	±0.539	±0.271	0.339	0.139	∓0.0214	1.008
	Present	±0.536	±0.269	0.349	0.116	∓0.211	0.996
	CLT	±0.539	±0.269	0.339	0.138	∓0.0213	1.000

[†] This form is drawn from (Pagano and Hatfield, 1972), Pagano's elasticity analytical solution (Pagano, 1972a,b), present hybrid stress shell element (6 × 6 mesh) and CLT (classical laminate theory).

and Liou and Sun (1987) using a three-dimensional hybrid stress method are compared in Table 2. Generally the predictions obtained by the present simple hybrid element are in good agreement with the analytical solution and the accuracy, and are similar to the one obtained by three-dimensional hybrid stress analysis with far more degrees of freedom.

4.2. *Bending of multiply square laminated plates* (a = b)

In this example, the multiply laminates are analysed with a view to examining the generality of the present element. This type of problem has been investigated also by Pagano and Hatfield (1972) for square bidirectional laminates of edge dimension a and thickness h consisting of three, five, seven and nine layers under the surface loading defined in eqn (26). The lamina material properties, normalized stresses and displacements are the same as in the previous problem [eqns (27) and (28)]. The material is assumed to be square-symmetric. All laminates considered are symmetric with respect to the central plane, the fiber orientations alternate between $0°$ and $90°$ with respect to the x axis, and the $0°$ layers are at the outer surfaces of the laminate. The total thickness of the $0°$ and $90°$ layers are the same, whereas layers at the same orientation have equal thicknesses.

Figure 4 shows the effect of different span–thickness ratios to the normalized central displacement for three layer plate. Certain aspects of the results predicted by the present element, as well as the analytical solutions (Pagano and Hatfield, 1972) and analogous CLT (Classical Laminate Theory) results are given in Tables 3–6 for various values of S. In a few instances (when the value of S is low) the maximum values of $\bar{\sigma}_{xz}$ and $\bar{\sigma}_{yz}$ do not occur at $z = 0$, hence in these cases there are two entries in the respective columns. The upper value gives the result at $z = 0$, while the lower number represents the maximum value, with the corresponding z being given in parentheses. For the three layers problem, the distribution of the normalized horizontal displacement $\bar{u}$ and normalized stress $\bar{\sigma}_x$, $\bar{\sigma}_{xz}$ and $\bar{\sigma}_{xy}$ through the thickness for $S = 4$ are shown in Figs 5(a)–(d), respectively. Using a zig-zag function in the inplane displacement approximation, excellent agreements between the present hybrid stress element and analytical elasticity solution are found for normalized inplane displacement $\bar{u}$, usually such an agreement can only be obtained by three-dimensional finite element analysis with far more degrees of freedom.

Because the continuity conditions of interlayer traction have been also relaxed in the present approach, the transverse shear stresses σ_{xz} and σ_{yz} are discontinuous at the interlayer surfaces, as shown in Fig. 5c, but the maximum shear stress can still be well-predicted by this method. In Fig. 6, the normalized horizontal displacement $\bar{u}$ of a nine-ply laminate for $S = 2, 4, 10$ are plotted. The accuracy of this hybrid stress model with increasing layers is confirmed again. Note that due to the fact that transverse normal stresses, σ_z, have been neglected in this approach, $\bar{u}$ is symmetric to the laminate midsurface as shown in Fig. 6, but there is no difficulty in taking σ_z into account by the present method.
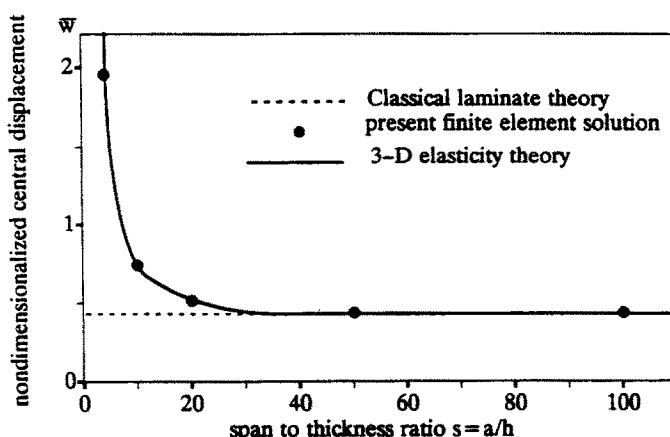

Fig. 4. Central deflection of three-layer (0/90/0) square plate.

Table 4. Maximum stresses and deflection in five-ply (0/90/0/90/0) laminate under sinusoidal loading†

$S = \dfrac{a}{h}$	Source	$\bar{\sigma}_x\left(\dfrac{a}{2},\dfrac{a}{2},\dfrac{h}{2}\right)$	$\bar{\sigma}_y\left(\dfrac{a}{2},\dfrac{a}{2},\dfrac{h}{3}\right)$	$\bar{\sigma}_{xz}\left(0,\dfrac{a}{2},0\right)$	$\bar{\sigma}_{yz}\left(\dfrac{a}{2},0,0\right)$	$\bar{\sigma}_{xy}\left(0,0,\dfrac{\pm a}{2}\right)$	$\bar{w}\left(\dfrac{a}{2},\dfrac{a}{2},0\right)$
4	Pagano	0.685	0.633	0.238	0.229	−0.0394	4.291
		−0.651	−0.626	0.238(0.02)	0.233(−0.11)	0.0384	
	Present	±0.651	±0.645	0.238	0.212	∓0.038	4.274
10	Pagano	±0.545	0.430	0.258	0.223	−0.0246	1.570
			−0.432		0.223(−0.02)	0.0247	
	Present	±0.540	±0.433	0.265	0.202	∓0.0242	1.552
20	Pagano	±0.539	±0.380	0.268	0.212	∓0.0222	1.145
	Present	±0.535	±0.379	0.277	0.190	∓0.0218	1.132
100	Pagano	±0.539	±0.360	0.272	0.205	∓0.0213	1.006
	Present	±0.535	±0.358	0.282	0.184	∓0.0210	0.994
	CLT	±0.539	±0.359	0.272	0.205	∓0.0213	1.000

† This form is drawn from (Pagano, 1972a,b). Pagano's elasticity analytical solution (Pagano, 1972a,b), present hybrid stress shell element (6 × 6 mesh) and CLT, (classical laminate theory).

Table 5. Maximum stresses and deflection in seven-ply (0/90/0/90/0/90/0) laminate under sinusoidal loading†

$S = \dfrac{a}{h}$	Source	$\bar{\sigma}_x\left(\dfrac{a}{2},\dfrac{a}{2},\dfrac{h}{2}\right)$	$\bar{\sigma}_y\left(\dfrac{a}{2},\dfrac{a}{2},\dfrac{3h}{8}\right)$	$\bar{\sigma}_{xz}\left(0,\dfrac{a}{2},0\right)$	$\bar{\sigma}_{yz}\left(\dfrac{a}{2},0,0\right)$	$\bar{\sigma}_{xy}\left(0,0,\dfrac{\pm a}{2}\right)$	$\bar{w}\left(\dfrac{a}{2},\dfrac{a}{2},0\right)$
4	Pagano	0.679	0.623	0.219	0.236	−0.0356	4.153
		−0.645	−0.610	0.223(0.12)		0.0347	
	Present	±0.643	±0.652	0.210	0.299	∓0.0338	4.110
10	Pagano	±0.548	0.457	0.255	0.219	−0.0237	1.529
			−0.458	0.255(−4.02)		0.0238	
	Present	±0.541	±0.462	0.234	0.276	∓0.0233	1.509
20	Pagano	±0.539	0.419	0.267	0.210	∓0.0219	1.133
			−0.420				
	Present	±0.535	±0.419	0.243	0.264	∓0.0216	1.120
100	Pagano	±0.539	±0.405	0.272	0.205	∓0.0213	1.006
	Present	±0.535	±0.402	0.256	0.168	∓0.0210	0.994
	CLT	±0.539	±0.404	0.272	0.205	∓0.0213	1.000

† This form is drawn from (Pagano, 1972a,b), Pagano's elasticity analytical solution (Pagano, 1972a,b), present hybrid stress shell element (6 × 6 mesh) and CLT (classical laminate theory).

Table 6. Maximum stresses and deflection in nine-ply (0/90/0/90/0/90/0/90/0) laminate under sinusoidal loading†

$S = \dfrac{a}{h}$	Source	$\bar{\sigma}_x\left(\dfrac{a}{2},\dfrac{a}{2},\dfrac{h}{2}\right)$	$\bar{\sigma}_y\left(\dfrac{a}{2},\dfrac{a}{2},\dfrac{2h}{5}\right)$	$\bar{\sigma}_{xz}\left(0,\dfrac{a}{2},0\right)$	$\bar{\sigma}_{yz}\left(\dfrac{a}{2},0,0\right)$	$\bar{\sigma}_{xy}\left(0,0,\dfrac{\pm a}{2}\right)$	$\bar{w}\left(\dfrac{a}{2},\dfrac{a}{2},0\right)$
4	Pagano	0.684	0.628	0.223	0.223	−0.0337	4.079
		−0.649	−0.612	0.223(0.01)	0.225(−0.06)	0.0328	
	Present	±0.645	±0.661	0.235	0.203	∓0.0318	4.032
10	Pagano	±0.551	0.477	0.247	0.226	−0.0233	1.512
					0.226(−0.01)	0.0235	
	Present	±0.544	±0.482	0.262	0.196	∓0.0229	1.490
20	Pagano	±0.541	±0.444	0.255	0.221	∓0.0218	1.129
	Present	±0.536	±0.444	0.272	0.190	∓0.0215	1.115
100	Pagano	±0.539	±0.431	0.259	0.219	∓0.0213	1.005
	Present	±0.535	±0.429	0.276	0.187	∓0.0210	0.994
	CLT	±0.539	±0.431	0.259	0.219	∓0.0213	1.000

† This form is drawn from Pagano (1972). Pagano's elasticity analytical solution (Pagano, 1972). Present: hybrid stress shell element (6 × 6 mesh). CLT (classical laminate theory).
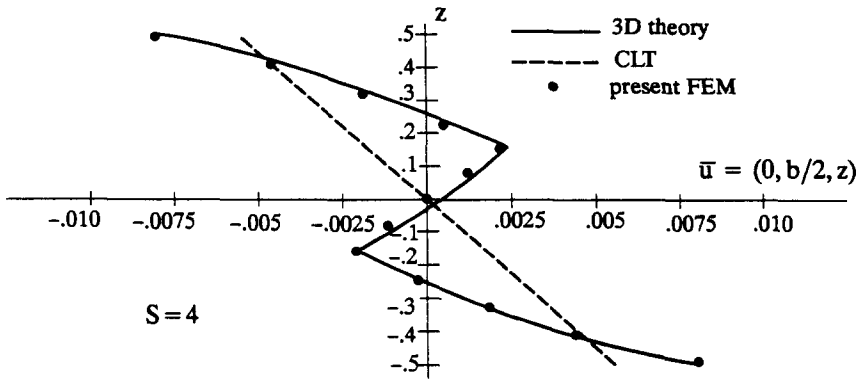
Y. K. CHEUNG and S. DI

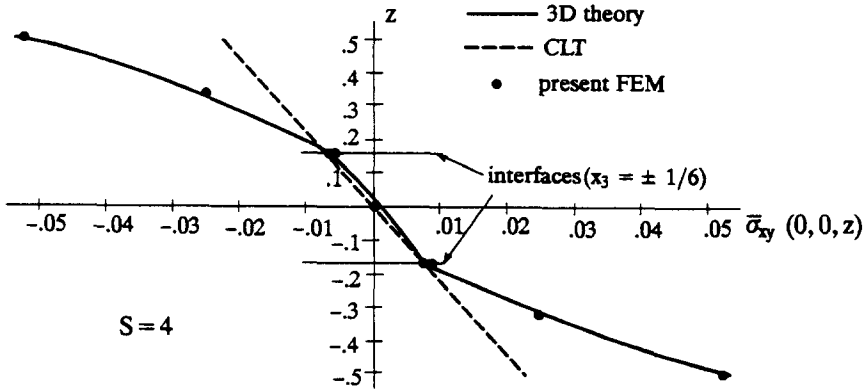Fig. 5(a). Inplane displacement ($a = b$, three-layer plate).

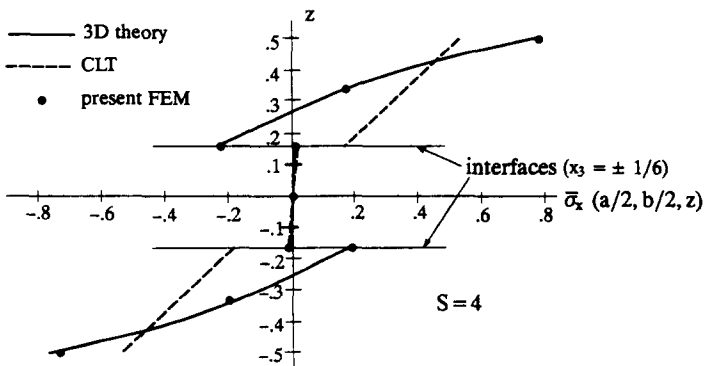Fig. 5(b). Inplane shear stress distribution ($a = b$, three-layer plate).

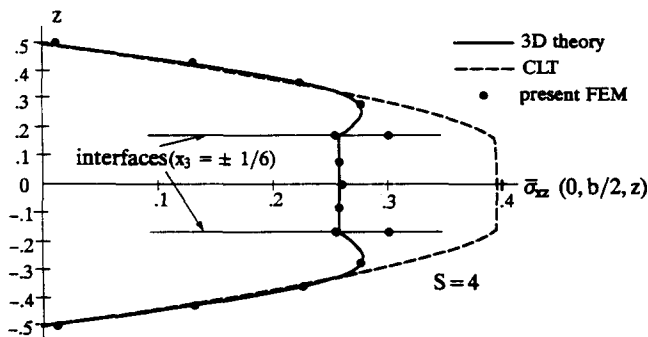Fig. 5(c). Normal stress distribution ($a = b$, three-layer plate).

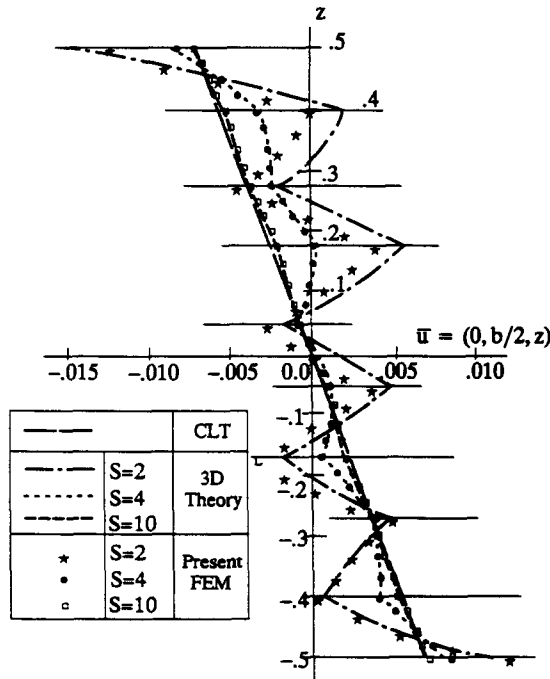Fig. 5(d). Transverse shear stress distribution ($a = b$, three-layer plate).

Fig. 6. Inplane displacement ($a = b$, nine-layer plate).

4.3. Angle ply ($\pm\theta$) laminates under uniform transverse loading

The final example problem considered here is a two layer laminate of angle ply ($\pm\theta$) construction, simply supported on all sides, and subjected to a uniformly distributed transverse load. For present purposes, only square plates are considered so that $a = b$ and a uniform 8×8 mesh is used for the entire plate, since fiber-orientation-induced bending/stretching coupling exists, which eliminates the usual (single layer) x–y plane symmetries. Results will be compared with a series solution (20 terms used here) given by Whitney (Whitney, 1970). Because that solution is based on lamination theory, it is evident from results presented earlier that only thin laminates ($L/h > 100$) can be analysed in the comparison. Here all the results are obtained for $a = b = 10$, $h = 0.02$, so that $S = L/h = 500$. In addition, layer material properties are :

$$\left.\begin{array}{l} E_L = 40 \times 10^6 \,\text{psi}, \qquad E_T = 10^6 \,\text{psi}, \\[2mm] G_{LT} = 0.5 \times 10^6 \,\text{psi}, \quad G_{TT} = 0.5 \times 10^6 \,\text{psi} \\[2mm] \nu_{LT} = \nu_{TT} = \nu_{TL} = 0.25. \end{array}\right\} \tag{29}$$

The midsurface transverse displacement w_o at the centre of the plate and midsurface inplane displacement u_o at $x = a/2$, $y = 0$, and v_o at $x = 0$, $y = b/2$ are listed in Table 6. The latter two quantities reflect the bending/stretching coupling for this unsymmetric laminate. Table 7 shows most quantities of interest are within 3% of the exact value for 8×8 mesh of the entire plate. Also we can find that θ has little effect on the accuracy of the predictions as mentioned by Spilker (1982).

5. CONCLUDING REMARKS

Hybrid stress four-node multilayer laminated plate element has been developed using a rational approach incorporating the energy constraint and higher-order shear deformation theory. Based on a modified Hellinger–Reissner principle, the equilibrium requirement for the assumed initial layer stress can be relaxed and the stress fields are pretreated by an energy constraint. The formulation can be used for the analysis of laminated plates consisting of

Table 7. Results for a thin simply supported square plate of $\pm\theta$ angle ply construction under uniform transverse load†

		$\pm5^\circ$	$\pm15^\circ$	$\pm25^\circ$	$\pm35^\circ$	$\pm45^\circ$
$u_o\left(\dfrac{a}{2},0\right)$	Whitney	0.2649	0.7710	1.135	1.465	1.481
	Present FEM	0.2525	0.7465	1.094	1.424	1.524
	Normalized value	(0.953)	(0.968)	(0.964)	(0.972)	(1.029)
$v_o\left(0,\dfrac{b}{2}\right)$	Whitney	1.871	3.281	2.502	1.161	1.481
	Present FEM	1.907	3.292	2.544	1.734	1.524
	Normalized value	(1.019)	(1.003)	(1.017)	(1.077)	(1.029)
$w_o\left(\dfrac{a}{2},\dfrac{b}{2}\right)$	Whitney	592.0	892.7	983.8	945.1	915.2
	Present FEM	592.3	894.32	983.2	950.1	925.6
	Normalized value	(1.001)	(1.002)	(0.999)	(1.005)	(1.011)

† Whitney's elasticity analytical solution (Whitney, 1970), present hybrid stress shell element (8×8 mesh).

an arbitrary number of layers without any difficulty. It is not necessary to use the shear correction factor and stress smoothing techniques, and the shear locking phenomenon no longer exists in the present hybrid element method. Through-thickness displacement fields incorporating with the zig-zag function have been used to model transverse shear deformation effects, by adding only two more degrees of freedom for each node.

The accuracy and efficiency of the present hybrid element have been verified by several examples. The present simple hybrid stress formulation can give rapid convergence and good accuracy, and in particular it can provide very satisfactory across thickness distribution for displacement and stress, which up to the present time could only be obtained by three-dimensional finite element analysis with many more degrees of freedom.

REFERENCES

Di, S. (1988). The optimization theory of numerical property for hybrid/mixed models and its applications. Ph.D. thesis, Southeast University, Nanjing, China (in Chinese).

Di, S. (1992). Higher-order laminated shell element and its application to nonlinear analysis. *Proceedings of the third Int. Conf. on Computational Plasticity, Fundamentals and Applications*, Barcelona, April 6–11, pp. 2059–2070, Pineridge.

Di, S. and Cheung, Y. K. (1991). On the hybrid/mixed finite element method with energy constraints. *Comput. Structs*, **41**, 461–474.

Di, S., Wu, C. and Song, Q. (1989). Model optimization of hybrid general shell element. *Acta Mech. Solida Sinica*, **2**, 1–18.

Di, S., Wu, C. and Song, Q. (1990). Optimization formulation of hybrid model for thin and moderately thickness plates. *Appl. Math. Mech.* **2**, 149–157.

Greenberg, J. B. and Stavsky, Y. (1980). Vibration of axially compressed laminated orthotropic cylindrical shells including transverse shear deformation. *Acta Mech.* **37**, 13–28.

Liou, W.-J. and Sun, C.T. (1987). A three-dimensional hybrid stress isoparametric element for the analysis of laminated composite plates. *Comput. Structs*, **25**, 241–249.

Mau, S. T. (1973). A simple higher-order theory for laminated composite plates, *J. Appl. Mech.* **40**, 606–607.

Mau, S. T., Tong, P. and Pian, T. H. H. (1972). Finite element solution for laminated thick plates. *J. Composite Mater.* **6**, 304–311.

Noor, A. K. and Andersen, C. M. (1977). Mixed isoparameteric finite element models of laminated composite shells. *Comput. Meth. Appl. Mech. Engng* **11**, 255–280.

Noor, A. K. and Rarig, P. L. (1974). Three-dimensional solutions of laminated cylinders. *Comput. Meth. Appl. Engng* **3**, 319–334.

Pagano, N. J. (1970a). Exact solutions for rectangular bidirection composites and sandwich plates. *J. Compos. Mater.* **4**, 20–34.

Pagano, N. J. (1970b). Influence of shear coupling in cylindrical bending of anisotropic plates. *J. Compos. Mater.* **4**, 330–343.

Pagano, N. J. and Hatfield, S. J. (1972). Elastic behavior of multilayered bidirectional composites. *AIAA Jl* **10**, 931–933.

Pian, T. H. H. (1964). Derivation of element stiffness matrices by assumed stress distribution. *AIAA Jl* **2**, 1333–1336.

Pian, T. H. H. and Chen, D. P. (1982). Alternative ways for formulation of hybrid stress elements. *Int. J. Numer. Meth. Engng* **18**, 1679–1684.

Pian, T. H. H. and Wu, C. (1988). A rational approach for choosing stress terms for hybrid element formulation. *Int. J. Numer. Meth. Engng* **26**, 2331–2343.

Reddy, J. N. (1984a). A simple higher-order theory for laminated composite plates. *J. Appl. Mech.* **51**, 745–752.

Reddy, J. N. (1984b). A note on symmetry considerations in the transient response of unsymmetrically laminated anisotropic plates. *Int. J. Numer. Meth. Engng* **20**, 175–194.

Reddy, J. N. and Chao, W. C. (1981). A comparison of closed-form and finite-element solutions of thick laminated anisotropic rectangular plates. *Nuclear Engng Des.* **64**, 153–167.

Reissner, E. and Stavsky, Y. (1961). Bending and stretching of certain types of heterogeneous aeolotropic plates. *J. Appl. Mech.* **28**, 402–408.

Spilker, R. L. (1982). Hybrid-stress eight-node elements for thin and thick multilayer laminted plates. *Int. J. Numer. Meth. Engng* **18**, 801–828.

Srinivas, S. and Rao, A. K. (1970). Bending, vibration and buckling of simply-supported thick orthotropic rectangular plates and laminates. *Int. J. Solids Structures* **6**, 1463–1481.

Whitney, J. M. (1969). The effect of transverse shear deformation on the bending of laminated plates. *J. Compos. Mater.* **3**, 534–547.

Whitney, J. M. (1970). The effect of boundary conditions on the response of laminated composites. *J. Compos. Mater.* **4**, 192–203.

Whitney, J. M. and Leissa, A. W. (1969). Analysis of heterogeneous anisotropic plates. *J. Appl. Mech.* **36**, 262–266.

Wu, C. and Bufler, H. (1990). Multivariable finite element: consistency and optimization. *China Sci.* **9**, 946–955.

Wu, C., Di, S. and Huang, M. (1987a). The optimization design of hybrid elements. *Kexue Tong-bao.* **32**, 1236–1239.

Wu, C., Di, S. and Pian, T. H. H. (1987b). Optimization formulation of hybrid stress axisymmetric elements. *Acta Aeronaut. Astronautic Sinica* **8**, A434–447 (in Chinese).